Chapter 5
A Numerical Study of Weak Lateral Dispersion in Discrete and Continuum Models

Luis A. Cisneros-Ake and Antonmaria A. Minzoni

Abstract We consider two dimensional discrete lattices with anharmonic interactions and weak transversal dispersion. We study the propagation of a continuum Kadomtsev-Petviashvili I lump and its semi discrete analogue and show the formation of caustics, due to the emission of linear waves, in both cases. We perform numerical experiments in different settings. We show how impurities and prestress can produce new lumps in analogy with one dimensional soliton formation in near critical flows.

5.1 Introduction

Effects of nonlinear interactions in the dynamics of discrete lattices in one and two space dimensions have been considered since the striking pioneering numerical experiments by Fermi, Pasta and Ulam (FPU) [5] in the middle of the last century. From the equipartition of energy and ergodicity to the existence and propagation of strongly localized structures (kinks, solitons, breathers or more generically Intrinsic Localized Modes) in anharmonic lattices has been the interest due to its relevance in a wide range of applications ranging from material science, nonlinear optics, physiology and biology to name a few [1, 3, 8, 9, 15, 16].

Discrete lattice systems are relevant in applications when the microscopic structure becomes relevant, nevertheless, their appropriate long wave limit reproduces the macroscopic phenomenology of the continuum medium of the models. There are however some aspects, like non Galilean invariance and the birth of the Peierls-Nabarro (PN) potential, that are inherent to the discrete systems that can only be

L.A. Cisneros-Ake (✉)
Department of Mathematics, ESFM, Instituto Politécnico Nacional,
Unidad Profesional Adolfo López Mateos Edificio 9, 07738 México D.F., México
e-mail: cisneros@esfm.ipn.mx

A.A. Minzoni
FENOMEC, Department of Mathematics and Mechanics, IIMAS, Universidad Nacional
Autónoma de México, Apdo 20-726, 01000 México, D. F., México
e-mail: tim@mym.iimas.unam.mx

studied in this limit. These kind of issues adds difficulties in the study of the dynamics of discrete lattices. The increasing of the space dimensions is another difficulty. For instance, it is well known in the literature that the one dimensional nonlinear Schrödinger (NLS) soliton ceases to exist when the space dimensions is increased [10], there are actually some time estimates, in terms of the space dimensions, for the blow up of localized structures.

We are interested in this chapter in the propagation of coherent structures(localized in space) in two dimensional lattices. This problem has been considered numerically in [2] on the electron transport and one of the questions is to examine the possibility of propagation of mechanical compressions, due to the presence of an electron for instance, in directions different to the crystallographic axes. Since localized excitations may percolate, depending on the mechanical excitation, in two dimensional crystal lattices in finite times leaving finite-length traces, the key point is then to find the mechanisms that could explain the define paths left by a moving localized structure and its persistence along the crystal. These issues are also related to the energy transport in solids and the tracks in mica, which is the main subject of this book. Our findings in this work show that a possible mechanism is to consider two dimensional semi discrete lattices which weakly laterally disperse.

Another set of problems is related to the effect of two dimensional impurities on the propagation of coherent structures. Finally the problem of the formation of coherent structures due to impurities in a prestressed lattice, which arises as the two dimensional analogue of soliton formation in supercritical flows past obstacles considered by Smyth [17], is also of interest. We study these type of questions in this work.

To begin the study of these questions we will introduce a Kadomtsev-Petviashvili (KP) type equation which will describe weak lateral dispersion in a lattice. This equation will be continuous in the direction of propagation and discrete in the orthogonal direction. We will assume an anisotropic lattice which in the linear regime oscillates around a minimum of the potential energy when the displacements of the particles are along the direction of propagation. On the other hand we will assume a bistable potential in the perpendicular direction. This gives two possible equilibria for the motion and an unstable equilibrium is between them.

Denote by $u_{n,m}(t) = u(n, m, t)$ the compressional displacement around the equilibrium in the n direction. We will have two contributions for the potential energy. The first one is $U(u_{n+1,m} - u_{n,m})$ where $U(r)$ has a minimum at $r = 0$. Along the discrete vertical direction the strain is given by $u(n, m + 1, t) - u(n, m, t)$ and we assume the energy in that direction, $V(r)$, to be a bistable potential with a maximum at $r = 0$. This gives for the total energy $U(u(n + 1, m, t) - u(n, m, t)) + V(u(n, m + 1, t) - u(n, m, t))$ which upon linearization takes the form: $\frac{\alpha^2}{2}(u(n + 1, m, t) - u(n, m, t))^2 - \frac{\beta^2}{2}(u(n, m + 1, t) - u(n, m, t))^2$. Thus the corresponding equation of motion takes the form

$$\ddot{u}_{n,m}(t) = \alpha^2 \left(u_{n+1,m} - 2u_{n,m} + u_{n-1,m} \right) - \beta^2 \left(u_{n,m+1} - 2u_{n,m} + u_{n,m-1} \right).$$
$$(5.1)$$

The linear dispersion relation for the mode $u_{n,m}(t) = e^{i(kn+lm-\omega t)}$ provides

$$\omega^2 = 4\alpha^2 \sin^2 \frac{k}{2} - 4\beta^2 \sin^2 \frac{l}{2}, \qquad (5.2)$$

where the sin l term takes into account the discrete nature of the lattice in the vertical direction. Clearly this dispersion relation is unstable for $k \ll l$. However, it is a standard approach to look for one directional waves with $l \ll k$ which have weak lateral dispersion. This expansion is valid for time scales shorter than the scale of the instability for a given choice of initial values. It provides a preliminary assessment of the weak lateral dispersion. This gives the KP I type equation as follows

$$\omega = \pm 2\sqrt{\alpha^2 \sin^2 \frac{k}{2} - \beta^2 \sin^2 \frac{l}{2}}. \qquad (5.3)$$

Assume $k \ll 1$, but keep $l \ll k$, to take into account the discrete effect in the m direction. Expanding to fourth order in k and assuming $\sin^2 \frac{l}{2} = O(k^4)$, we obtain

$$\omega = \alpha k - \frac{\alpha}{24} k^3 - \frac{2\beta^2}{\alpha k} \sin^2 \frac{l}{2} \qquad (5.4)$$

which is the linear dispersion relation for the linear KP I equation in the form, often moving with linear phase velocity α,

$$u_{xt} + \alpha u_{xx} + \frac{\alpha}{24} u_{xxxx} - \frac{\beta^2}{2\alpha} \left(u(x, m+1) - 2u(x, m) + u(x, m-1) \right) = 0. \quad (5.5)$$

When nonlinearities in $U(u_x)$ are considered, it is well established that the consistent nonlinear correction is of the KdV type. This gives a generic term $\gamma(u_x)u$ which often differentiation gives the semi discrete KP I equation in the form:

$$u_{xt} + u_{xxxx} + 6(u_x u)_x - 3 \left(u(x, m+1) - 2u(x, m) + u(x, m-1) \right) = 0, \quad (5.6)$$

where we transformed this equation into standard form by considering an appropriate coordinate system and by taking $\frac{\beta^2}{2\alpha} = 3$, $\frac{\alpha}{24} = 1$ and $\gamma = 6$. Equation (5.6) describes the effect of weak discrete lateral dispersion in a localized disturbance in a lattice. The lattice is unstable to lateral disturbances but in the KP limit, for the continuum case, the instability is satisfied by the nonlinear effect forming a stable lump solution. We would like to study the effect of discrete dispersion in this context. The long wave limit in the $y = m$ direction of (5.6) gives the KP I equation:

$$u_{xt} + u_{xxxx} + 6(u_x u)_x - 3u_{yy} = 0. \qquad (5.7)$$

We recall [17] that the lump solution for the KP I equation (5.7) is given in the form:

$$u(x, y, t) = 2\frac{\partial^2}{\partial x^2} \log\left[(x' + ay')^2 + b^2 y'^2 + \frac{1}{b^2} \right] = 4 \frac{-(x' + ay')^2 + b^2 y'^2 + \frac{1}{b^2}}{\left[(x' + ay')^2 + b^2 y'^2 + \frac{1}{b^2} \right]^2}$$

(5.8)

where $x' = x - 3(a^2 + b^2)t$ and $y' = y + 6at$ for free real parameters a and b. Thus, the velocity of the lump is $v = \sqrt{v_x^2 + v_y^2}$ where $v_x = 3(a^2 + b^2)$ and $v_y = -6a$.

We end presenting the organization of this chapter. In the next section we describe the numerical method used in the numerical experiments. We then consider wave propagation in the semi discrete and continuum KP I to show, using ray's theory, the caustic's formation due to the emission of linear radiation of a traveling lump profile. The third section is devoted to the numerical study of discrete structures moving along the transverse direction and the dynamics of lump interaction. We also consider in this section the lump interaction with impurities or obstacles in both the semi discrete and continuum KP I. In the fourth section we study the elastic lattice analogue of the problem of critical flow past obstacles. We provide a very preliminary interpretation based on the fundamental work of [17]. We present our conclusions in the last section.

5.2 Numerical Approximation to the Kadomtsev-Petviashvili I Equation

We follow reference [4] to propose a second order central finite difference approximation in space and an implicit Crank-Nicolson to also get a second order approximation in time. To this end, we define the finite difference operators [11]:

$$D_{+,x} f_j = \frac{1}{\Delta x}(f_{j+1} - f_j) = f'(x_j) + O(\Delta x),$$

$$D_{0,x} f_j = \frac{1}{2\Delta x}(f_{j+1} - f_{j-1}) = f'(x_j) + O(\Delta x^2),$$

$$D_x^2 f_j = \frac{1}{\Delta x^2}(f_{j-1} - 2f_j + f_{j+1}) = f''(x_j) + O(\Delta x^2),$$

$$D_x^4 f_j = \frac{1}{\Delta x^4}(f_{j+2} - 4f_{j+1} + 6f_j - 4f_{j-1} + f_{j-2}) = f''''(x_j) + O(\Delta x^2),$$

where $f_j = f(x_j)$ and $x_j = j\Delta x$. We thus get the finite difference scheme for (5.7) in the form:

$$D_{0,x} D_{+,t} u_{n,m}^l + D_x^2((3u^2)_{n,m}^l + (3u^2)_{n,m}^{l+1}) + D_x^4(u_{n,m}^l + u_{n,m}^{l+1}) - 3D_y^2(u_{n,m}^l + u_{n,m}^{l+1}) = 0,$$

(5.9)

where $u^l_{n,m} = u(x_n, y_m, t_l) = v(n\Delta x, m\Delta y, l\Delta t)$. Equation (5.9) provides an implicit non linear algebraic system of equations for the unknowns $u^{l+1}_{n,m}$ provided the previous values $u^l_{n,m}$ are known for $l = 0, 1, ...$ where $u^0_{n,m}$ corresponds to the initial condition at $t = 0$. One should solve the non linear system (5.9) using, for example, a Newton method every time step. One can, however, linearize (5.9) using Taylor's expansions in Δt by keeping the second order approximation of the overall scheme. Doing this, we may approximate the nonlinear part $(3u^2)^l_{n,m} + (3u^2)^{l+1}_{n,m} = 6u^{l+1}_{n,m}u^l_{n,m} + O(\Delta t^2)$. We now rearrange (5.9) as a linear system for the unknowns $u^{l+1}_{n,m}$:

$$A^l\mathbf{u}^{l+1} = \mathbf{d}^l \tag{5.10}$$

where the mth entries of the previous vector identity are given by:

$$a^l_{n,m}u^{l+1}_{n,m-1} + b^l_{n,m}u^{l+1}_{n-2,m} + c^l_{n,m}u^{l+1}_{n-1,m} + g^l_{n,m}u^{l+1}_{n,m}$$
$$+e^l_{n,m}u^{l+1}_{n+1,m} + b^l_{l,m}u^{l+1}_{n+2,m} + a^l_{l,m}u^{l+1}_{n,m+1} = d^l_{n,m}$$

with coefficients given by:

$$a^l_{n,m} = -3q, \quad b^l_{n,m} = r, \quad c^l_{n,m} = 6pu^l_{n-1,m} - 4r - 1,$$
$$g^l_{n,m} = 6r - 12pu^l_{n,m} + 6q, \quad e^l_{n,m} = 6pu^l_{n+1,m} - 4r + 1,$$
$$d^l_{n,m} = u^l_{n+1,m} - u^l_{n-1,m} - r(u^l_{n+2,m} - 4u^l_{n+1,m} + 6u^l_{n,m} - 4u^l_{n-1,m} + u^l_{n-2,m})$$
$$+ 3q(u^l_{n,m+1} - 2u^l_{n,m} + u^l_{n,m-1}),$$

and $p = \Delta t/\Delta x, q = \Delta t \Delta x/\Delta y^2, r = \Delta t/\Delta x^3$. The authors of [4] have checked that the linearized implicit finite difference scheme for the KP I equation is unconditionally linearly stable. In practice, however, we must take sufficiently small steps Δx, Δy and Δt to handle nonlinear stability. In [4] it is also shown that the numerical dispersion, induced by central finite differences in the spatial derivatives, is second order in space and time therefore the numerical dispersion does not exceed the physical dispersion. Finally, for the numerical implementation of the finite difference method we consider numerical boundary conditions of the Neumann type: $u^l_{-N-2,m} = u^l_{-N-1,m} = u^l_{-N,m}, u^l_{N,m} = u^l_{N+1,m} = u^l_{N+2,m}$ for $m = -M, ..., M$ and $u^l_{n,-M-1} = u_{n,-M}, u^l_{n,M+1} = u^l_{n,M}$ for $n = -N, ..., N$.

5.2.1 Continuous and Discrete Lump Propagation

In Fig. 5.1a we reproduce the evolution of the continuum lump like initial condition (5.8), which is not exactly satisfied in the parameters a and b, to show the readjustment to an exact lump by shedding backwards radiation, and confining it
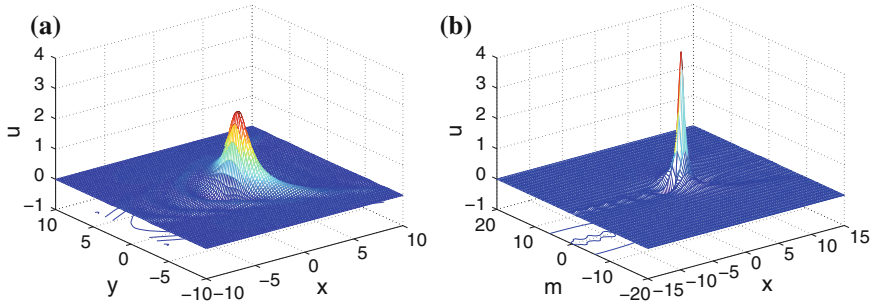
Fig. 5.1 Linear dispersed radiation in **a** continuum KP I for $\Delta x = \Delta y = 0.2$ and **b** semi discrete KP I for $\Delta x = 0.2$, $\Delta y = 1$ both at $t = 0.5$ and wave parameters $a = 0$, $b = 1$, $x_0 = y_0 = 0$

inside a parabolic caustic continuum lump like initial conditions in [14]. It is to be noted that the linear radiation is shed backwards since the group velocity is negative.

In Fig. 5.1b we display the discrete analogue of the continuum solution shown in previous Fig. 5.1a. We consider a quite wide lump oriented in the continuous x direction as an initial condition for the semi discrete system (5.6). We observe that as time evolve the lump narrows down substantially to half the original width due to the transverse discreteness. This thinning is accompanied by a very narrow tail of radiation moving backwards and in the forward direction the radiation is confined by a parabolic caustic similar to the continuum one (see [14]).

We explain the shrinking of the soliton as induced by the confinement of the radiation and the PN potential induced by the lattice. We now explain using the linear theory the mechanism for the confinement of the radiation which is quite different in the two cases.

5.2.1.1 Caustic Formation and Radiation Confinement

The linear radiation emitted by the KP I (5.7) for non exact lump solutions traveling along the x-axis, in the continuum limit, satisfies the linearised KP equation [14]:

$$\frac{\partial^2 u}{\partial x \partial t} + \frac{\partial^4 u}{\partial x^4} - 3\frac{\partial^2 u}{\partial y^2} = g(x - \xi(t), y, t), \tag{5.11}$$

where $g = -(u_{0t} + 6u_0 u_{0x} + u_{0xxx})_x + 3u_{0yy}$ is the forcing due to the approximate lump $u_0 = u_0(x - \xi(t), y, t)$. For the caustic formation, the form of g is not needed explicitly since the solution of the forced equation (5.11) is as a superposition of linear modes in the form:

$$u(x, y, t) = \frac{1}{4\pi^2} \int\limits_{-\infty}^{\infty} \int\limits_{-\infty}^{\infty} G(k, l)e^{i[k(x-\xi(t))+ly-\omega(k,l)t]}dkdl, \tag{5.12}$$

where the dispersion relation $\omega(k, l)$ for the linear equation (5.11) is $\omega(k, l) = -k^3 - 3\frac{l^2}{k}$. We now consider the phase $\psi(k, l) = k(x - \xi(t)) + ly - \omega(k, l)t$ and we make use of the stationary phase approximation to find the main contribution of the integral (5.12). The stationary values of the phase $\psi(k, l)$ are attained at $\psi_k(k, l) = 0$ and $\psi_l(k, l) = 0$. We thus find

$$0 = \psi_k(k, l) = x - \xi(t) - \omega_k t = x - \xi(t) + \left(3k^2 - 3\frac{l^2}{k^2}\right)t,$$

$$0 = \psi_l(k, l) = y - \omega_l t = y + 6\frac{l}{k}t.$$

We find from last equation $\frac{l}{k} = -\frac{y}{6t}$ and substitute back into the first of the last equations to obtain the family of planar curves:

$$F(x - \xi(t), y, k) = x - \xi(t) + \left(3k^2 - \frac{y^2}{12t^2}\right)t = 0, \qquad (5.13)$$

as the equation which gives the family of real rays emanating from the source at $x = \xi(t)$. The radiation is then confined by the envelope of the rays given by $F_k = 0$. This gives $k = 0$ and the parabolic caustic in the form:

$$x = \xi(t) + \frac{y^2}{12t}. \qquad (5.14)$$

This expression, since is singular at the initial time $t = 0$, shows that a parabolic caustic is formed instantly at the front of the lump.

For the semi discrete KP I equation (5.6), the situation is quite different. The linear radiation for the KP I equation continuum in the x-axis and discrete in the $y = m$ direction satisfies the linear equation

$$\frac{\partial^2 u_m}{\partial x \partial t} + \frac{\partial^4 u_m}{\partial x^4} - \frac{3}{h^2}(u_{m-1} - 2u_m + u_{m+1}) = g(x - \xi(t), m, t), \qquad (5.15)$$

for $u_m = u_m(x, t)$ and lattice spacing h in the y-axis. A similar argument as before shows that the solution to the linearized semi-discrete equation (5.15) is given by:

$$u_m(x, t) = \frac{1}{4\pi^2} \sum_{m=-\infty}^{\infty} \int_{-\infty}^{\infty} G(k, l)e^{i[k(x - \xi(t)) + lmh - \omega(k, l)t]}dk, \qquad (5.16)$$

where the dispersion relation $\omega(k, l) = -k^3 - \frac{12}{kh^2}\sin^2\left(\frac{lh}{2}\right)$. The phase now is $\psi(k, l) = k(x - \xi(t)) + lm - \omega(k, l)t$ and the stationary phase theorem gives:

$$0 = \psi_k(k, l) = x - \xi(t) + \left(3k^2 - \frac{12}{k^2 h^2} \sin^2\left(\frac{lh}{2}\right)\right) t$$

$$= x - \xi(t) + \left(3k^2 - \frac{6}{k^2 h^2}(1 - \cos(lh))\right) t,$$

$$0 = \psi_l(k, l) = m + \frac{12}{kh} \sin\left(\frac{lh}{2}\right) \cos\left(\frac{lh}{2}\right) t = m + \frac{6}{kh} \sin(lh) t.$$

Last equation provides $\sin(lh) = -\frac{mkh}{6t}$ which in turn simplifies first of last equations in the form:

$$0 = F(x - \xi(t), m, k) = \psi_k(k, l) = x - \xi(t) + \left(3k^2 - \frac{6}{k^2 h^2}\left(1 - \sqrt{1 - \frac{m^2 k^2 h^2}{36t^2}}\right)\right) t. \tag{5.17}$$

Again this gives a family of rays whose envelope is the caustic. Now the envelope for the caustic is found solving simultaneously last equation and

$$0 = F_k(x - \xi(t), m, k) = k^4 + 2 + \frac{-2 + \frac{m^2 k^2 h^2}{36t^2}}{\sqrt{1 - \frac{m^2 k^2 h^2}{36t^2}}}. \tag{5.18}$$

Now this equation has two branches of solutions one for $k = 0$ and the second one for $k = k(m, t)$. This when substituted into (5.17) gives the actual caustic. This is plotted in Fig. 5.2. This shows that unlike the continuum problem the radiation is confined to the region A defined by the caustics. This explains the narrow tail of radiation observed in Fig. 5.1b (see level curves at the bottom of this figure).

Fig. 5.2 Caustics in the continuum (5.14) (*dot-dashed curve*) and in the semi discrete (5.17)–(5.18) (*continuous curve*) for $h = 1$ both at $\xi = 0$ and $t = 1$
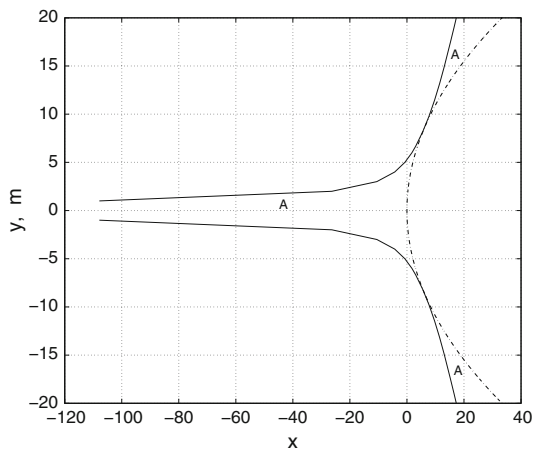
5.3 Lateral Motion and Interaction of Pulses with Obstacles

We begin by considering an oblique lump propagating upwards in the m direction. Figure 5.3 shows the numerical evolution of an initial wide lump. We may see how the PN makes a thin lump in the m direction and how the lump is being pinned by the PN in the m direction allowing propagation in the x direction only. If one enlarges one of Fig. 5.3b or Fig. 5.3c, one may see that the lump is centered between discrete sites on m, say in Fig. 5.3b the lump is centered at $m = 2.5$ and in Fig. 5.3c the lump is centered at $m = 4.5$. This is expected in lattice systems since at the middle of sites the PN attains its minimum. So that, the general picture for propagation along the discrete variable m is that the lump hops from site to site and eventually stops in one of them because of the PN potential. The continuous direction x allows the lump to move in that direction. Our last observation about this numerical evolution is on the parabolic front. We may see how the parabolic front tries to preserve its form on the direction of propagation, this is in concordance with the caustic's formation as it was discussed previously.
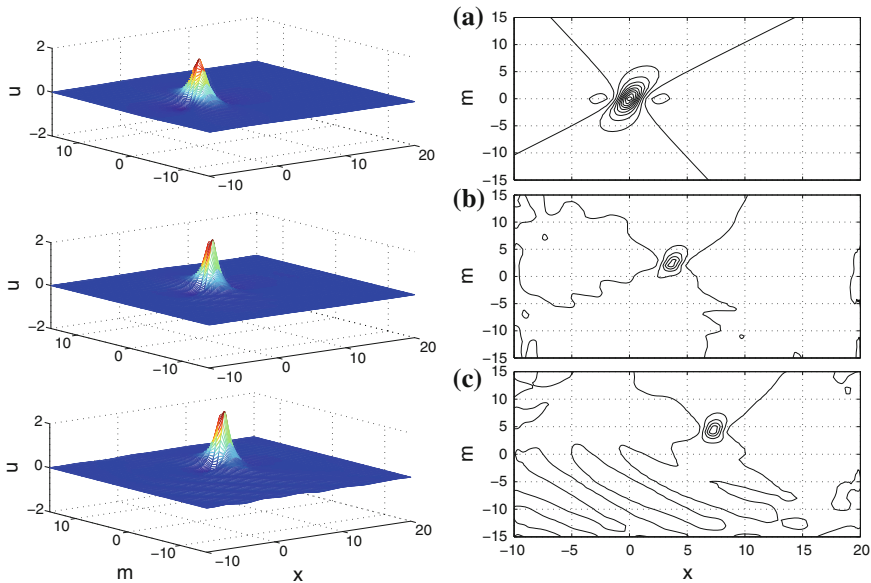

Fig. 5.3 Oblique propagation: Full numerical solution of semi discrete KP I (5.6) for $\Delta x = 0.1$, $\Delta y = 1$, $\Delta t = 0.02$ at **a** $t = 0$, **b** $t = 2$ and **c** $t = 4$. The lump profile (5.8) is used as initial condition for $a = -0.25$, $b = 0.7$, $x_0 = y_0 = 0$
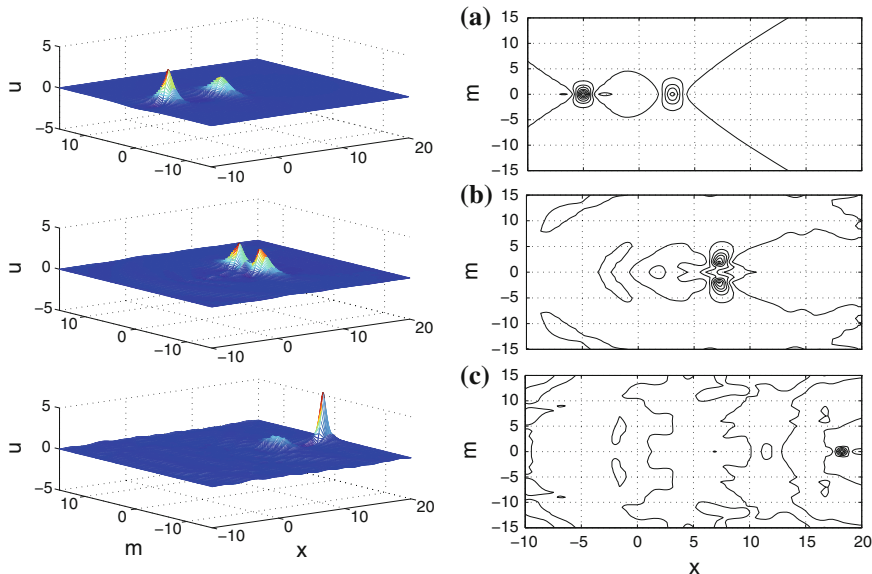
Fig. 5.4 Direct collision: Full numerical solution of semi discrete KP I (5.6) for $\Delta x = 0.1$, $\Delta y = 1$, $\Delta t = 0.02$ at **a** $t = 0$, **b** $t = 2.5$ and **c** $t = 5$. Lump profiles (5.8) are used as initial condition for $a = 0$, $b = 1$, $x_0 = -5$, $y_0 = 0$ and $a = 0$, $b = 0.75$, $x_1 = 3$, $y_1 = 0$

We may also see the linear dispersed radiation moving with the appropriate group velocity and confined by the narrow caustic at the back of the pulse. This is in agreement with the linear result for a source moving obliquely.

To study the interaction of pulses we recall that the continuum KP I lump interaction exhibits a very complicated evolution. For direct collision along the x-axis it is known that the lumps, after the collision, form symmetric lumps on the y-axis that later become together to reconstruct the two lumps on the x-axis [6, 13]. We now see how this phenomenon takes places in our semi discrete KP I equation. We see from Fig. 5.4 a similar phenomenon as the one just explained before in the continuous case. The only difference is that the reconstruction of the lumps after the collision is not so perfect due to the PN effect. The faster lump is reconstructed as a still much faster lump which is thiner and higher in form. The opposite occurs to the slower lump.

We finally consider the effect of an obstacle, which in the present context can be considered as the compression/expansion caused by an external impurity, in both the continuous (5.7) and semi discrete (5.6) KP I equations. The effect of the obstacle is
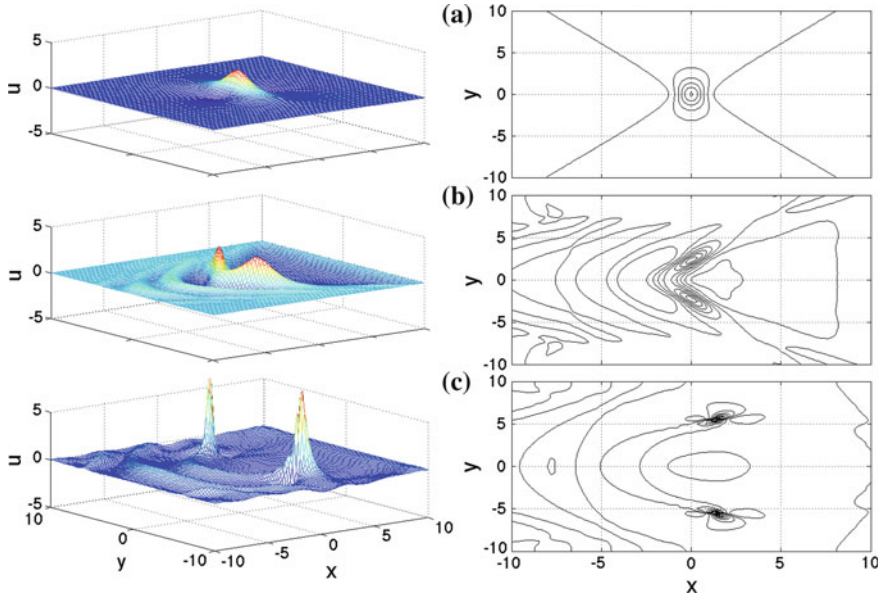
Fig. 5.5 Lump with obstacle down ($f_1 = -0.1$ at R_1: $0 \le x \le 1$, $-0.5 \le y \le 0.5$ and $f_2 = 0$ at R_2): Full numerical solution of KP I (5.7) for $\Delta x = \Delta y = 0.2$, $\Delta t = 0.02$ at **a** $t = 0$, **b** $t = 0.74$ and **c** $t = 1.5$. The lump profile (5.8) is used as initial condition for $a = 0$, $b = 0.8$ and $x_0 = y_0 = 0$

considered as a right hand side $f(x, m)$ and $f(x, y)$ in (5.6) and (5.7), respectively. The obstacle f is zero almost every where except in the domains R_1 and R_2 where it takes values f_1 and f_2, respectively.

In Fig. 5.5 we show a lump colliding with an obstacle centered in the x axis. We observe that it splits symmetrically into two lumps which then overtake the obstacle traveling along the parabolic continuum caustic. We can think of the splitting as analogous to the splitting produced upon the collision of two pulses previously studied. It is to be noted that the radiation of the two pulses, as expected, merge and travels backwards with the appropriate group velocity.

In Fig. 5.6 we show the effect of discreteness in the current problem. The impurities are located in a small region of the positive x axis at $m = 0$. Again the initial pulse splits but now the first two symmetric pulses that are born apparently travel almost perpendicularly to the direction of propagation. The motion along the continuous x axis of the daughter lumps is now much slower than the vertical motion. The backwards moving radiation, which give place to the birth of lumps, is now confined to a narrow region, as it was described in the second section.
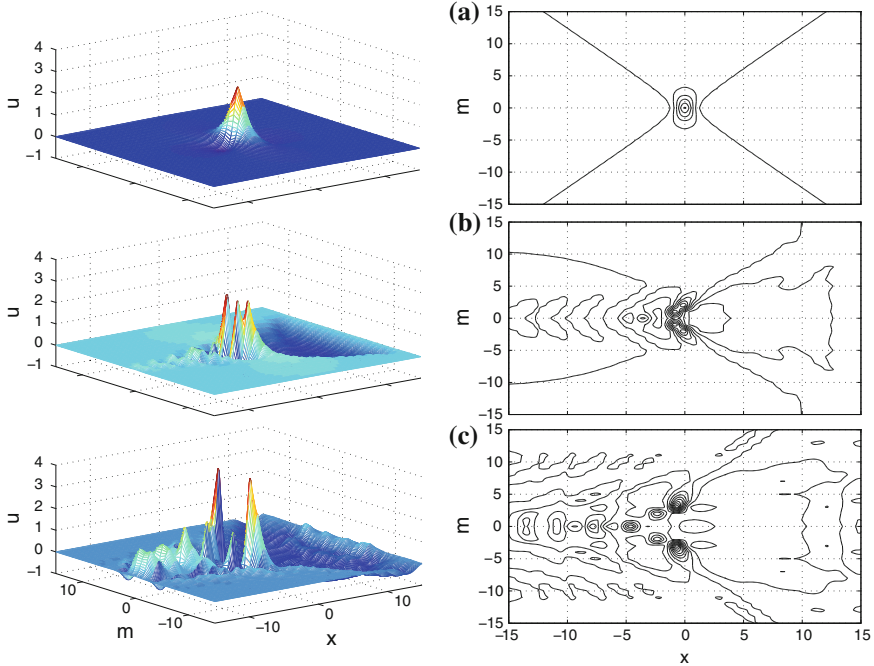
Fig. 5.6 Lump with obstacle down ($f_1 = -0.1$ at R_1: $0 \leq x \leq 0.5$, $m = 0$ and $f_2 = 0$ at R_2): Full numerical solution of discrete KP I (5.6) for $\Delta x = 0.1$, $\Delta y = 1$, $\Delta t = 0.02$ at **a** $t = 0$, **b** $t = 0.74$ and **c** $t = 1.5$. The lump profile (5.8) is used as initial condition for $a = 0$, $b = 0.8$ and $x_0 = y_0 = 0$

5.4 The Effect of Impurities in a Prestressed Lattice

We consider the analogue of the problem of resonant flow impinging on an obstacle forming undular bores as studied in [17] for the KdV equation. It must be remarked that in [7] the two dimensional analogue of [17] in the KP II equation was numerically studied in this context. It was found numerically in [12] that the modulated wave train in the continuum KP I is now deformed into a modulated train of lump solitons produced by the main flow impinging on the obstacle which evolve along the caustic. We study the same problem for the lattice, which is discrete in the transverse direction, and the continuous KP I. To this end, we replace u by $u + U$ and t by δt into (5.6) and (5.7) to obtain KP I analogues of the forced KP II studied in [7],
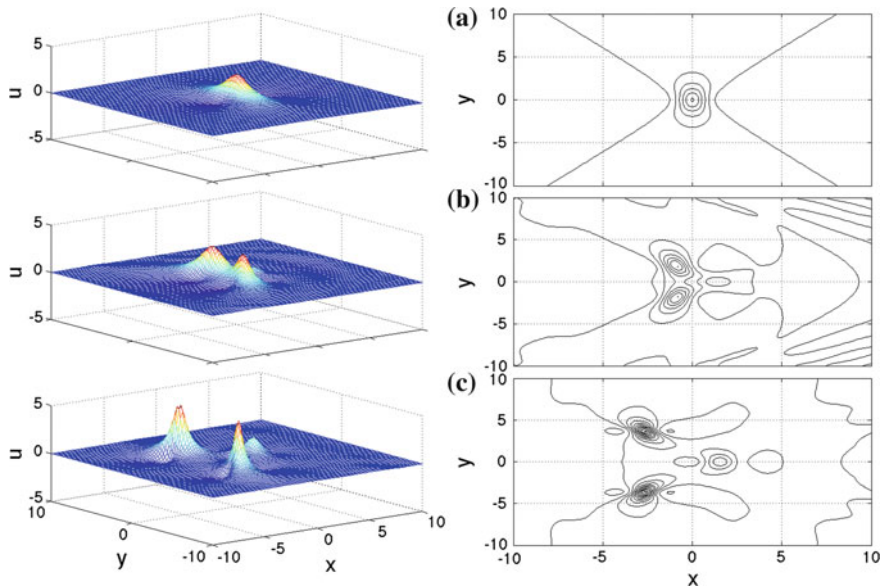
Fig. 5.7 Lump with obstacle up/down ($f_1 = 0.1$ at R_1: $0 \le x \le 1$, $-0.5 \le y \le 0.5$ and $f_2 = -0.1$ at R_2: $1 \le x \le 2$, $-0.5 \le y \le 0.5$) and constant flux $U = -0.5$ and $\delta = -1$: Full numerical solution of KP I (5.20) and $\Delta x = \Delta y = 0.2$, $\Delta t = 0.02$ at **a** $t = 0$, **b** $t = 1$ and **c** $t = 2$. The lump profile (5.8) is used as initial condition for $a = 0$, $b = 0.8$ and $x_0 = y_0 = 0$

$$\delta \frac{\partial^2 u_m}{\partial x \partial t} + 6U \frac{\partial^2 u_m}{\partial x^2} + 3 \frac{\partial^2 u_m^2}{\partial x^2} + \frac{\partial^4 u_m}{\partial x^4} - 3\left(u_{m-1} - 2u_m + u_{m+1}\right) = f(x, m) \tag{5.19}$$

and

$$\delta u_{xt} + 6U u_{xx} + 3\left(u^2\right)_{xx} + u_{xxxx} - 3u_{yy} = f(x, y) \tag{5.20}$$

respectively. The constant U is the state of constant deformation while the forcing compression $f(x, m)$ or $f(x, y)$ is the external localized compression (or topography impurities) which is being imposed on the deformed lattice and it is assumed to be placed instantaneously.

The first problem we consider is the one of evolution of a lump in a prestressed lattice. In Fig. 5.7 we consider the effect of the first obstacle in the continuum case. We observe the lump colliding with obstacle. As a result the lump splits. Two large lumps are reflected with large velocity and a smaller lump is transmitted. This behavior can be explained using the previous result of lump interaction. We have to the leading
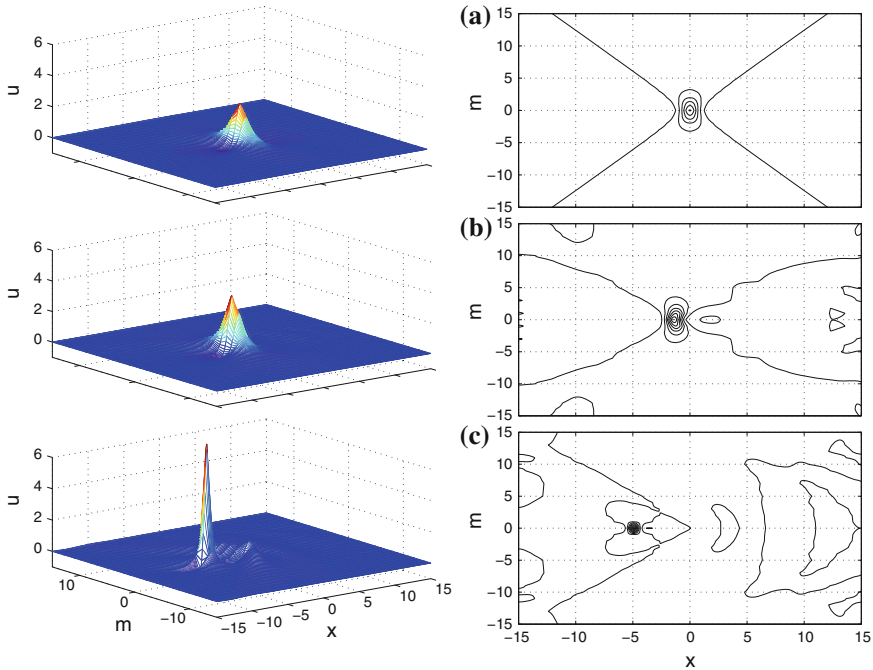
Fig. 5.8 Lump with obstacle up/down ($f_1 = 0.1$ at R_1: $0 \le x \le 0.5$, $m = 0$ and $f_2 = -0.1$ at R_2: $0.5 \le x \le 1$, $m = 0$) and constant flux $U = -0.5$ and $\delta = -1$: Full numerical solution of discrete KP I (5.19) and $\Delta x = 0.1$, $\Delta y = 1$, $\Delta t = 0.02$ at **a** $t = 0$, **b** $t = 1$ and **c** $t = 2$. The lump profile (5.8) is used as initial condition for $a = 0$, $b = 0.8$ and $x_0 = y_0 = 0$

edge of the lump interactions with the obstacle producing a backwards moving wave since the obstacle acts as a source. This wave interacts with the main lump playing the same role as a pulse which splits the pulse and each piece is swept backwards by the flow induced by the obstacle.

In Fig. 5.8 we have the same situation for the discrete case. The behavior is different. Now the pulse is just bounced back leaving a narrow tail of radiation; no splitting is observed. Now the PN potential prevents the splitting and the backward flow produced by the object reflects the pulse which after hitting the obstacle travels to the left. The small radiation shed of the pulse is confined in the narrow caustic while the radiation at the back is confined by the parabolic caustic.
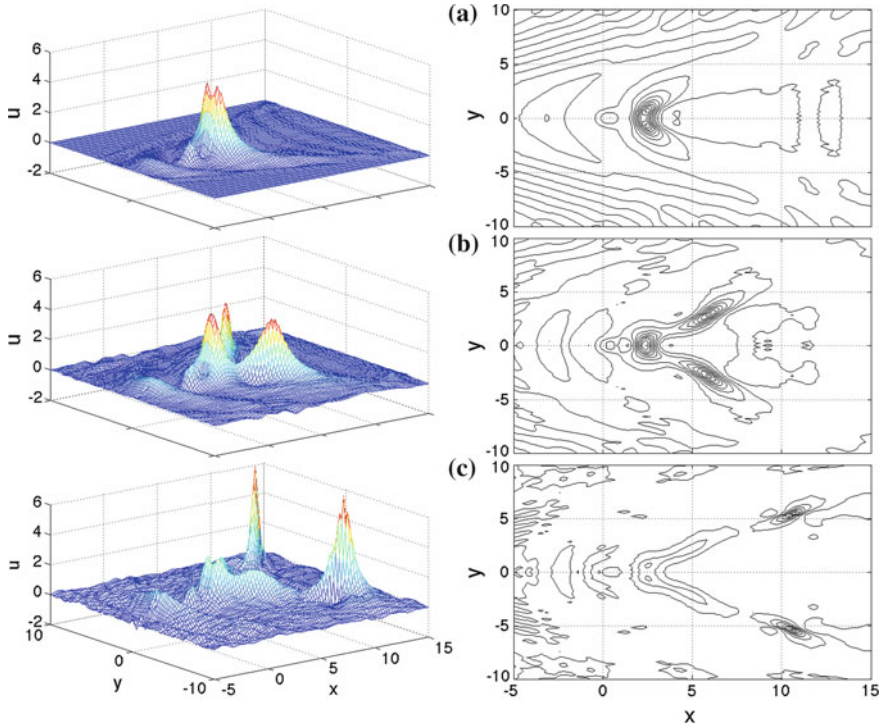
Fig. 5.9 $u = 0$ at $t = 0$ with obstacle up/down ($f_1 = 0.25$ at R_1: $0 \leq x \leq 1$, $-0.5 \leq y \leq 0.5$ and $f_2 = -0.25$ at R_2: $1 \leq x \leq 2$, $-0.5 \leq y \leq 0.5$) and constant flux $U = 0.5$ and $\delta = 1$: Full numerical solution of KP I (5.20) and $\Delta x = \Delta y = 0.2$, $\Delta t = 0.02$ at **a** $t = 0.5$, **b** $t = 1$ and **c** $t = 1.5$

We finish this section by considering a positive flow U passing an obstacle from zero initial conditions in u. We show in Fig. 5.9 the creation of a family of lump solitons emerging from the obstacle, due to the constant flow U, and moving along the caustic in the continuum. We may see that it takes some time after other pair of symmetric lumps are generated after the previous ones. Due to our computer limitations we are just able to see some of them, it takes longer times to see the complete evolution. This figure reproduces the main result obtained in [12]. The semi discrete counterpart is quite similar. Figure 5.10 shows the lump generation due to a positive flow through an obstacle in a semi discrete medium. The only difference with respect to the continuum, as expected, is the effect of the second caustic in the discrete KP I that influences the creation and the direction of motion in the family of lumps.
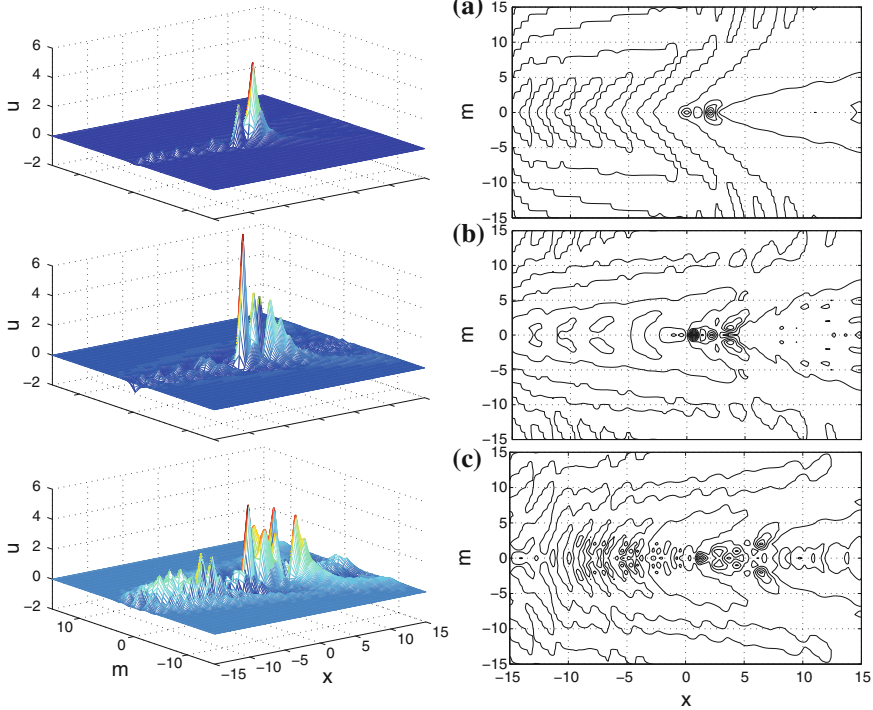
Fig. 5.10 $u = 0$ at $t = 0$ with obstacle up/down ($f_1 = 0.25$ at R_1: $0 \leq x \leq 0.5$, $m = 0$ and $f_2 = -0.25$ at R_2: $0.5 \leq x \leq 1$, $m = 0$) and constant flux $U = 0.5$ and $\delta = 1$: Full numerical solution of discrete KP I (5.19) and $\Delta x = 0.1$, $\Delta y = 1$, $\Delta t = 0.02$ at **a** $t = 0.4$, **b** $t = 0.8$ and **c** $t = 1.2$

5.5 Conclusions

We have shown that the effects of weak lateral dispersion in a two dimensional lattice can be described by a KP I type equation in the case of a bistable potential between lattice sites in the direction transverse to the main propagation direction. We have shown how the discreteness of the lattice narrows the width of the continuum lump. Moreover we have explained the radiation pattern of the evolving semi discrete lump in terms of a double caustic for the linear radiation.

We have also studied how discreteness changes the oblique propagation by pinning the lump in the transverse direction allowing it to move parallel to the crystal axis. The effect of obstacles was studied numerically and was shown to provide a guiding mechanism for lumps along the caustic of the linear waves produced by the obstacle. This shows how lumps could be guided in direction transverse to the crystallographic axis by introducing impurities appropriately. It will be of interest to study the effect of different impurities arranged as to guide lump solitons in different directions to reach various lattice points and thus allow prescribed percolations.

It also remains to be studied the coupling of a semi discrete KP with an NLS type equation to explore the existence of supersonic solectrons [18] in two dimensional lattices.

References

1. Assanto, G.: Nematicons: Spatial Optical Solitons in Nematic Liquid Crystals. John Wiley and Sons (2013)
2. Chetverikov, A.P., Ebeling, W., Velarde, M.G.: Controlling fast electron transfer at the nanoscale by solitonic excitations along crystallographic axes. Eur. Phys. J. B **85**, 291 (2012)
3. Davydov, A.S.: Solitons in Molecular Systems. Reidel, Dordrecht (1991)
4. Feng, B.F., Mitsui, T.: A finite difference method for the Korteweg-de Vries and the Kadomtsev-Petviashvili equations. J. Comp. Appl. Math. **90**, 95 (1998)
5. Fermi, E., Pasta, J., Ulam, S.M.: Studies of nonlinear problems. I. Technical Report LA-1940, Los Alamos Scientific Laboratory (1955). Also in Amaldi, E., et al. (eds.) Enrico Fermi: Collected papers. Vol. II, University of Chicago Press, pp. 850 (1965)
6. Gorshkov, K., Pelinovsky, D.E., Stepanyants, Y.A.: Normal and anormal scattering, formation and decay of bound states of two-dimensional solitons described by the Kadomtsev- Petviashvili equation. JETP **77**, 237 (1993)
7. Katsis, C., Akylas, T.R.: On the excitation of long nonlinear water waves by a moving pressure distribution. Part 2. Three-dimensional effects. J. Fluid. Mech. **177**, 49 (1987)
8. Keener, J., Sneyd, J.: Mathematical Physiology. Springer, New York (1998)
9. Kittel, C.: Introduction to Solid State Physics. John Wiley and Sons, New York (2005)
10. Kuznetsov, E.A., Rubenchik, A.M., Zakharov, V.E.: Soliton stability in plasmas and hydrodynamics. Phys. Rep. **142**, 103 (1986)
11. LeVeque, R.J.: Finite difference methods for ordinary and partial differential equations. SIAM (2007)
12. Lu, Z., Liu, Y.: The generation of lump solitons by a bottom topography in a surface-tension dominated flow. Z. Naturforsch **60a**, 328 (2005)
13. Manakov, S.V., Zakhorov, V., Bordag, L.: Two-dimensional solitons of the Kadomtsev-Petviashvili equation and their interaction. Phys. Lett. **63**, 205 (1977)
14. Minzoni, A.A., Smyth, N.F.: Evolution of lump solutions for the KP equation. Wave Motion **24**, 291 (1996)
15. Moloney, J.V., Newell, A.C.: Nonlinear Optics. Westview Press, New York (2003)
16. Murray, J.D.: Mathematical Biology I: An introduction. Springer, New York (2002)
17. Smyth, N.F.: Modulation theory solution for resonant flow over topography. P. Roy. Soc. Lond. B Bio. **409**, 79 (1987)
18. Velarde, M.G.: From polaron to solectron: the addition of nonlinear elasticity to quantum mechanics and its possible effect upon electric transport. Comp. Appl. Math. **233**, 1432 (2010)